

Fabrication and Characterization of ZnO Nanosheet on a Silver-metalized Polyimide Substrate

Alper Cetinel 

Ege University, Department of Physics, Izmir, Turkey

ABSTRACT

ZnO nanosheets were fabricated on a silver-metalized polyimide (PI/Ag) substrate using electrochemical deposition. FE-SEM, XRD, UV-Vis absorption, and I-V measurements were employed to examine the structural, optical and electrical properties of silver-metalized PI film and ZnO deposited PI/Ag film. For a comparison, PI/Ag film was also investigated without ZnO layer. FE-SEM analysis indicated that a silver film layer, consisted of spherical Ag nanoparticles, and the ZnO nanosheets were synthesized on PI substrate by electroless and electrochemical deposition, respectively. Moreover, the growth mechanism of the Ag film and ZnO nanosheets was also discussed. The characterization of X-ray diffraction verified that the ZnO nanosheets had a hexagonal phase and grew along the [002] direction. The optical absorbance spectra of bare PI, PI/Ag, and PI/Ag/ZnO showed a broad absorption peak around 300 nm. The electrical properties of the PI/Ag and PI/Ag/ZnO samples were studied by current-voltage (I-V) measurements in the dark environment at room temperature (300 K). The I-V measurements suggested that the samples presented ohmic characteristics. The results revealed that the deposition of ZnO on PI/Ag substrate improved the electrical conductivity compare with bare PI/Ag.

Keywords:

ZnO nanosheet; Polyimide; Silver; Electrochemical deposition; SEM; XRD; Characterization

Article History:

Received: 2021/07/19

Accepted: 2022/02/07

Online: 2022/03/30

Correspondence to: Alper Cetinel, Ege University, Department of Physics, 35030, Bornova, Izmir, Turkey.
E-Mail: alper.cetinel@ege.edu.tr
Phone: +90 (232) 311 2372

INTRODUCTION

As flexible optoelectronic materials develop increasingly common, there is a significant demand for flexible conducting electrodes, which are crucial parts for optoelectronic devices [1–3]. Polymer-based materials are the most widely used candidates for flexible substrate due to their benefits of high flexibility, low-cost and easy processability [4]. Among them, polyimide (PI) are the most promising flexible substrate materials thanks to their high heat resistance, superior mechanical properties and high radiation resistivity [5–7]. Though, the adhesion of passive metals, such as silver, nickel, copper, to polymers is very weak [8]. To enhance the surface adhesion of polyimide, many techniques are usually carried out such as chemical deposition methods, sputtering deposition methods, electrochemical deposition, and electroless deposition [4]. Among them, electrochemical and electroless depositions allow the growth of metal nanostructures on polymeric films, without changing the properties of the films [9]. Moreover, these methods are variable owing to uncomplicated materials, light reaction conditions, and applicability to non-conductive surfaces.

Silver has the highest conductivity (10^7 S/m) among noble metals and also has outstanding reflectivity at longer wavelengths [1]. The PI/silver film could present many advantages in flexibility and elasticity [9, 10]. Akamatsu et al. [11] reported that polyimide films have been prepared in silver nitrate solution by the electroless method. The metalized polyimide was obtained through both excellent conductivity and reflectivity [11]. However, the chemical stability of the flexible polyimide substrate is reduced considerably, as a result of the catalysed decay of polyimide chains (carbon bonds) by silver, hence, limit their practical applications. To passivate PI surface, carbon nanotube and metal nanoparticles (NPs), such as Pt, Ni and Cu were used up to now [12–15]. In addition, there are several reports on the use of ZnO on PI substrate [1, 16–20]. In recent years, the formation of ZnO seed and/or buffer layers on polymer substrates has been commonly used to fabricate ZnO nanorod or nanosheet layers on substrates [20]. Although the seed/buffer layers are useful for producing ZnO nanostructures, there are some challenges concerning device functionality. The most important issue is the production cost. Compared to other production

methods, the electrochemical deposition method is a simple, fast, low-cost process. Moreover, it provides the ability to tailor size, shape, and morphology of the nanostructures deposited under a set of well controlled synthesis parameters. To the best of our knowledge, there are no reports so far about the electrochemical deposition of ZnO nanosheet on a silver-metallized polyimide (PI/Ag) substrate.

In this study, as the first step, the surface of polyimide was chemically adjusted applying potassium hydroxide (KOH) to produce potassium polyamate. Then silver nanostructures were formed on polyimide substrate via the electroless deposition. In final step, ZnO nanosheet layer has been prepared on silver metallized PI substrate by electrochemical deposition without using any seed/buffer layer. The structural, optical, and electrical analyses were performed with a field emission scanning electron microscopy (FE-SEM), X-ray diffraction (XRD), ultraviolet–visible (UV–Vis) absorption and I-V measurements.

MATERIAL AND METHODS

All chemicals employed in this research were purchased from Sigma-Aldrich® and Polyimide substrate was obtained from DuPont (Kapton HN, 75 μm thick). The details of the procedure used for the PI surface adjustment shown in Figure 1. First, A PI substrate was cleaned with acetone and isopropanol, and washed with distilled water. Then, the PI substrate was immersed into a 5 M KOH solution at 50 °C for 5 min. As a result of this process, potassium polyamate was formed on the PI surface via cleavage of their imide rings [11, 21, 22]. Then, surface metallization of PI film was carried out by dipping of PI film in 5 mM silver nitrate (AgNO_3) and 0.17 M glucose solution for 15 min at room temperature (Electroless deposition). An ion-exchange process occurred between K^+ ions in PI film and silver ions during the electroless deposition.

PI/Ag sample was annealed at 300 °C for 30 min in vacuum furnace. After thermal treatment, ZnO nanosheets were obtained by electrochemical deposition technique. The deposition solution contained of an aqueous solution of 0.05M $\text{Zn}(\text{NO}_3)_2 \cdot 6\text{H}_2\text{O}$ and 0.05 M $\text{C}_6\text{H}_{12}\text{N}_4$. The pH and temperature were selected as 5.1 and 80 °C, respectively. The anode and cathode electrode were a PI/Ag film and platinum wire, respectively. ZnO nanosheets were deposited on PI/Ag at a constant current density of 0.5 mA/cm^2 for 30 minutes. After the deposition, PI/Ag/ZnO was washed with distilled water. Figure 2 shows the digital images of the samples obtained after electroless and electrochemical deposition. Surface morphologies of PI/Ag and PI/Ag/ZnO samples were examined with FE-SEM (QuantaFEG). X-ray diffraction (XRD) patterns were obtained from a

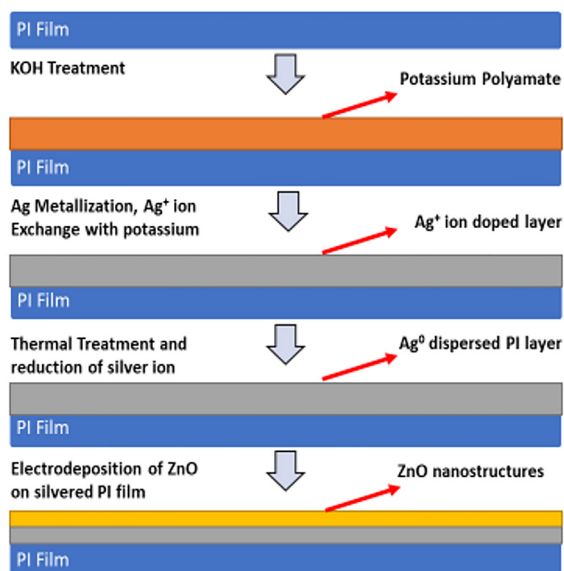


Figure 1. Schematic representation of the surface modification of the polyimide film and electrochemical deposition of ZnO on PI/Ag film.

Panalytical Empyrean XRD system using a CuK_α radiation ($\lambda = 0.15418 \text{ nm}$). The absorption spectra of samples were obtained using a Perkin Elmer Lambda 950 (UV/Vis/NIR) spectrophotometer within the range of 200–800 nm. The forward and reverse bias I-V measurements were performed using Keysight B2901A source meter (SMU) in dark at room temperature (300 K).

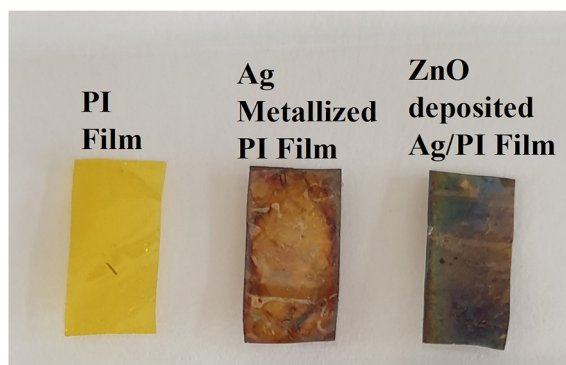


Figure 2. Digital images of the surface morphologies of the PI films before and after metallization of Ag and ZnO deposited, respectively.

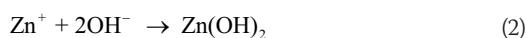
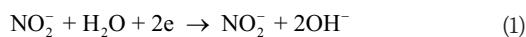
RESULTS AND DISCUSSION

SEM Analysis

As illustrated in Figure 1, before forming homogeneous ZnO nanostructures, PI film was embedded in AgNO_3 solution to form the Ag film on top of the PI surface to increase the chemical and electrical stability. Then, ZnO layer was formed on the PI/Ag substrate. Ag layer acts as a nucleation site for the ZnO layer growth. The Ag particles forming after the metallization of PI film and ZnO deposited PI/Ag sample were characterized using the

secondary electron mode in FE-SEM to provide topographical and elemental information. Figure 3 (a) shows a top surface FE-SEM image of PI/Ag. As seen in Figure 3 (a), the layer of Ag particles developed on PI film after the electroless deposition. Moreover, the Ag layer is homogeneous with respect to morphology and nanoparticle diameter. The average diameter of spherical Ag nanoparticle is about 200 nm. It has also found that smaller spherical silver nanoparticles coalesce and form silver nanorods that grow upwards from the surface (Figure 3 (a)). The growth process of Ag structures could be described by diffusion-limited aggregation (DLA) model [23]. Initially, Ag⁺ ions take electrons to create silver particles on the PI which was treated with KOH. As the reaction continue, the further silver particles are produced at the same time. At the end of process, Ag film (nanorod and spherical particles), formed by agglomerated Ag nanoparticles, is obtained on the PI surface.

Figure 3 (b) demonstrates the FE-SEM image of ZnO structures grown on PI/Ag at 80 °C and indicates that obtained structures consist of sheet-like structure. As seen in Figure 3 (b), the ZnO nanosheets are linked to each other and produce networks on the Ag nanoparticles. The average thickness of the ZnO nanosheets are in the range of 500-1000 nm with the typical diameter of 1–5 μm. Mostly the ZnO nanosheets are combined to form flower-shaped patterns. Recent studies reveal that the influence of deposition parameters such as current density, solution temperature and pH values, on the growth of ZnO nanostructures are significant [24]. The SEM analysis results are consistent with the works conducted by Aydemir et al. [24] and Yang et al. [25]. To explain growth of ZnO nanosheet via electrochemical deposition, the possible chemical reactions that take place are as shown below [25]:



In the case of the growth of ZnO nanosheet layer on PI/Ag, at the initial stage of deposition, smaller ZnO nanoparticles were formed on PI/Ag film. It is important to note that the formation of ZnO nanoparticles is critical because it requires nucleation spots for nanosheet creation. Then, a lot of ZnO nuclei produced and combined. As the process continues, the individual groups ultimately expand into nanosheets. Accumulations of smaller particle groups would subsequently establish larger clusters, which has promoted the formation of the sheet-like structure [25].

The composition of the prepared samples was studied further by conducting EDAX analysis. Figure 4 shows the

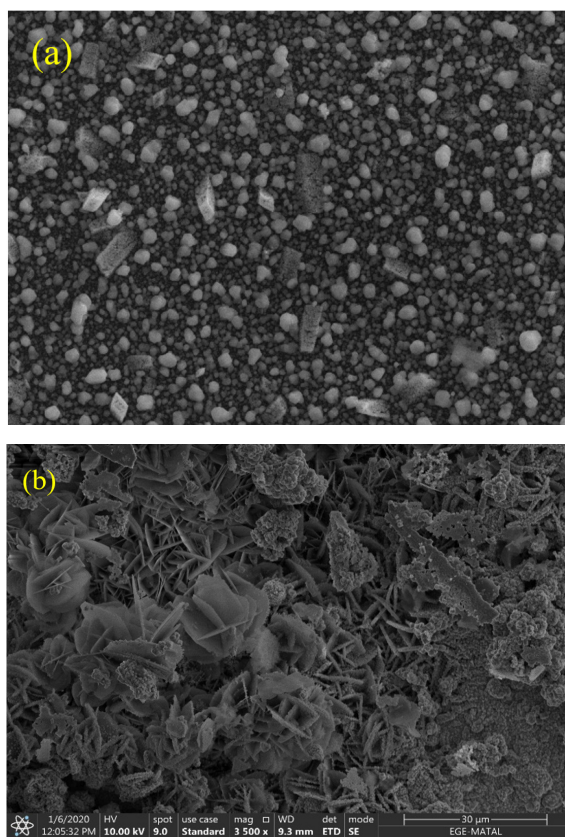


Figure 3. (a) FE-SEM image of silver nanostructures on PI substrate after electroless deposition (b) FE-SEM image of ZnO nanosheet on PI/Ag substrate after electrochemical deposition.

EDAX profiles of the PI/Ag and PI/Ag/ZnO samples. During the electroless deposition PI substrates in the AgNO₃ solution, ion-exchange is estimated to occur between K⁺ and Ag⁺ ions. EDAX spectra in Figure 4 a,b indicate that Ag and O are detected but also a negligible detection of K. The slightly low K atomic percentage is attributed to above-mentioned immersion process. It is also estimated that oxygen is formed because of the formation of a carboxylate function with K⁺ counter ions. Figure 4 c,d shows the EDAX spectra of PI/Ag sample after deposited ZnO. It is revealed that K⁺ is no more detected while ZnO is detected. At the surface of the PI/Ag, ion-exchange could be occurred between K⁺ and Zn²⁺ ions during the electrochemical deposition on the surface of PI/Ag substrate. Furthermore, increase of the oxygen atomic percentage is probably due to the imide cycle hydrolysis.

XRD Analysis

X-Ray diffraction was presented to examine and identify the purity of phase and the structure of the samples. Figure 5 represents the XRD patterns of silver metalized PI film and ZnO deposited PI/Ag sample. The XRD patterns of silver metalized PI film indicated that the obtained structure of Ag nanoparticle is face-centered cubic (FCC). As shown in Figure 5 (a), XRD analysis of PI/Ag

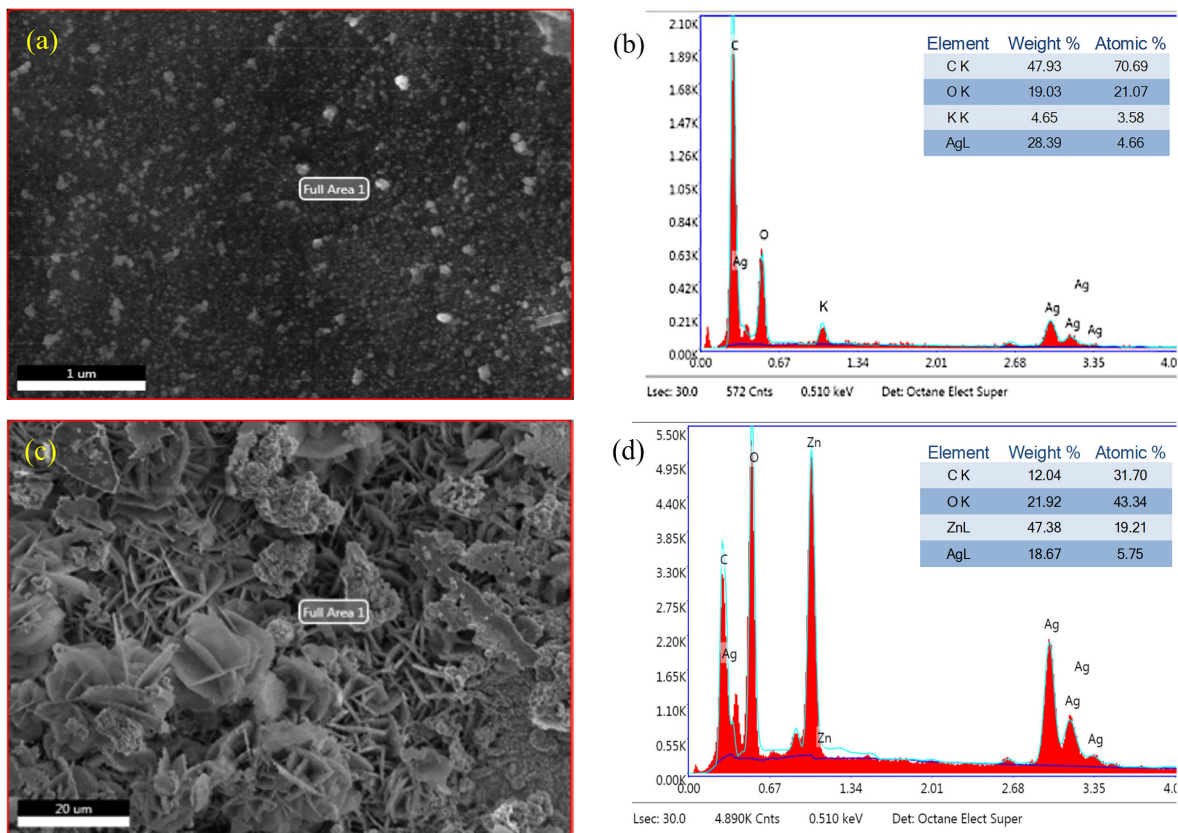


Figure 4. (a)-(b) EDAX analysis of silver nanostructures on PI substrate after electroless deposition, (c)-(d) EDAX analysis of ZnO nanosheet on PI/Ag substrate after electrochemical deposition.

sample reveals that three diffraction peaks at 2θ values of 38° , 44° , and 62° are attributed to the (111), (200), and (220) planes of the FCC structure of silver, which is consistent with the JCPDS file no. 4-0781 [22, 25]. Despite the Ag diffraction peaks, the peak observed at 20° belongs to the PI substrate [18]. XRD analysis clearly shows that Ag nanoparticles have a preferred orientation along the [111] direction.

Figure 5 (b) indicates the XRD pattern of the ZnO nanosheets obtained on PI/Ag. The peaks at 2θ values of 32° , 34° , 36° , and 47° correspond to (100), (002), (101), and (102) planes of the wurtzite structure of ZnO (JCPDS No. 36-1451) [25]. As seen in Figure 5 (b), the XRD pattern of the PI/Ag/ZnO demonstrates axis orientation along (002). It is clearly understood that the growth pattern is along the c-axis. XRD analysis of PI/Ag/ZnO indicates that the grown ZnO nanosheets represent a hexagonal wurtzite crystalline structure [16,24,25]. As seen in Figure 5 (b), apart from the (002) plane, additional small peaks in the XRD pattern of the PI/Ag/ZnO sample confirms the existence of the polycrystalline ZnO.

The average crystallite size of the PI/Ag and PI/Ag/ZnO samples along (111) and (002) planes was estimated using Scherrer formula (Eq. 4), using full width at half

maximum (FWHM) [26],

$$D = \frac{0.9\lambda}{\beta \cos\theta} \quad (4)$$

where D , λ , β and θ are the crystallite size, the wavelength of incident X-ray (1.5418 \AA), FWHM of the (111) and (002) peaks and the diffraction angle, respectively. From the Scherrer equation, the average crystallite size of Ag nanoparticles for the PI/Ag and PI/Ag/ZnO samples are about 30.5 and 26.8 nm, respectively. The average crystallite size of ZnO nanosheet along (002) planes calculated from Scherrer equation is about 41.5 nm.

Optical Measurements

The optical absorption spectra of Ag and ZnO embedded PI film are demonstrated in Figure 6. The absorption spectra of bare PI film are also added for reference. As seen in Figure 6, the absorption edge of PI film is at 230-260 nm range. After Ag and ZnO deposition, the absorption edge is shifted to the longer wavelengths. The absorption spectra of Ag and ZnO embedded PI film are shown in the range of 200–400 nm, and the absorption was reduced above 400 nm. In the spectrum of the PI/Ag/ZnO, the absorption peak appeared about 300 nm, is the

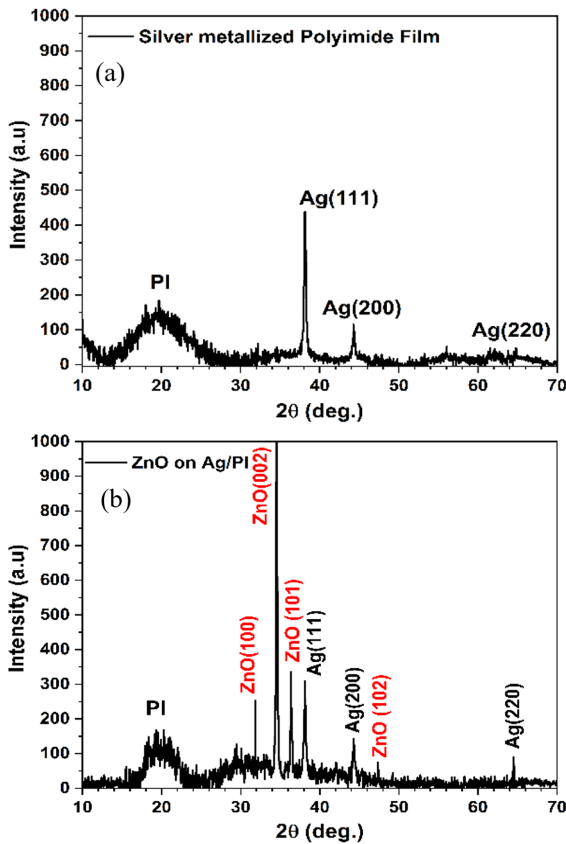


Figure 5. (a) XRD patterns of PI/Ag, (b) XRD patterns of PI/Ag/ZnO.

characteristic peak correspond to the exciton absorption of ZnO. It should be noted that for the sample of PI/Ag, there is not observed any absorption peak at about 400 nm, corresponding to the surface plasmon resonance (SPR) in silver nanostructures, because of the formation of discontinuous but interconnected Ag nanorods layer [23, 27].

I-V Measurements

The electrical properties of the all samples were investigated by measuring the current-voltage (I-V) characteristic at room temperature (300 K) and in the dark environment. These measurements were made using Keysight B2901A Source Meter (SMU) in the bias range of -5V to + 5V. Figure 7 shows I-V plots of silver metallized PI film and ZnO deposited PI/Ag sample.

As seen in Figure 7, these structures exhibit non-rectifying property and show an ohmic characteristic. Low sheet resistance and linear I-V behaviour are vital for the efficiency and reliability of flexible semiconductor devices, and their synthesis and characterization are considerable efforts in circuit fabrication [19]. Therefore, the bulk resistance (R) of the samples could be determined from Figure 7 (V/I) [28]. The electrical resistance of PI/Ag and PI/Ag/

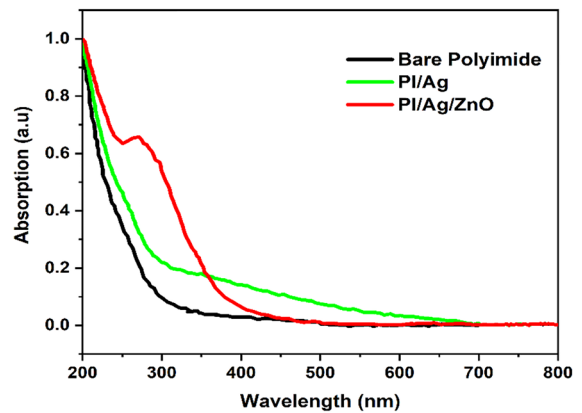


Figure 6. Optical absorption spectra of the bare PI film, PI/Ag and PI/Ag/ZnO samples.

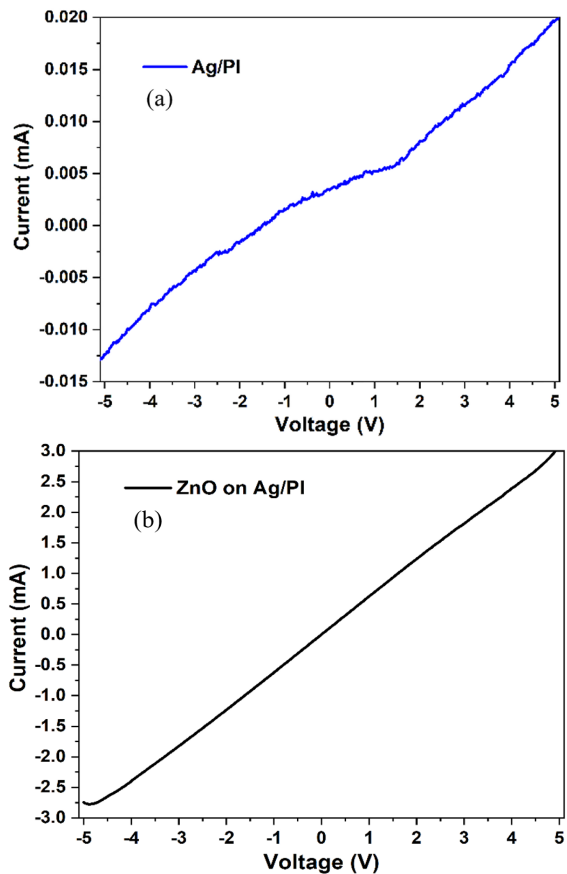


Figure 7. Dark current versus voltage characteristic of the samples at room temperature (a) PI/Ag, (b) PI/Ag/ZnO.

ZnO samples are calculated as 252 k Ω and 1.67 k Ω . Also, a four-point probe is used to determine the sheet resistance of samples. The Rs of PI/Ag and PI/Ag/ZnO samples are calculated as 884.45 k Ω /sq and 294.30 k Ω /sq. The high of sheet resistance of the PI/Ag sample is probably due to the presence of unbonded potassium ions on the PI surface after electroless deposition, which was also observed in SEM-EDAX analyses. The absence of these potassium ions in EDAX analysis after ZnO deposition revealed that ZnO passivated the PI/Ag surface and helped to reduce both

bulk resistance and sheet resistance.

CONCLUSION

In conclusion, surface modification and silver metallization of polyimide (PI) film were successfully performed by immersion method and ZnO were deposited onto surface of PI for passivation purpose by electrochemical deposition. The structural and electrical properties of silver metallized PI film and ZnO deposited PI/Ag film have been investigated by FE-SEM, XRD and I-V measurement. FE-SEM analysis revealed that after the electroless deposition, an Ag film layer consisted of spherical Ag nanoparticle was formed on the surface of the PI film. The average diameter of spherical Ag nanoparticles is about 200 nm. FE-SEM analysis indicated that ZnO nanosheets were successfully fabricated by electrochemical deposition on PI/Ag film. The average thickness of the ZnO nanosheets are in the range of 500-1000 nm. The XRD analysis shows that for PI/Ag sample, the obtained structure of Ag nanoparticle was face-centered cubic (FCC) and Ag nanoparticles were oriented in the (111) direction. XRD analysis of ZnO deposited PI/Ag film indicates that ZnO nanosheets had hexagonal wurtzite crystalline structure and were oriented in the [002] direction. The optical absorption spectra were measured in the range from 200 nm to 800 nm, and the absorption peaks for bare PI, PI/Ag and PI/Ag/ZnO appeared around 250–300 nm. The current-voltage (I-V) analysis was carried out to examine the electrical properties of the PI/Ag and PI/Ag/ZnO samples in the dark environment at room temperature (300 K). The I-V measurements suggested that the samples exhibited ohmic characteristics. Also, the results of I-V measurements were clearly indicated that deposited ZnO passivated the PI/Ag surface and improved electrical conductivity. Consequently, the ZnO deposited PI/Ag could be a good candidate for the possible applications in optoelectronic and sensor devices.

CONFLICT OF INTEREST

I do not have any conflict of interest or common interest with any institution or person that I know that could affect my work.

References

1. Lee D, Youn DY, Luo Z, Kim I D. Highly flexible transparent electrodes using a silver nanowires-embedded colorless polyimide film via chemical modification. *RSC Adv.* 6 (2016) 30331–30336.
2. Yu Y, Shen W, Li F, Fang X, Duan H, Xu F, Xiong Y, Xu W, Song W. Solution-processed multifunctional transparent conductive films based on long silver nanowires/polyimide structure with highly thermostable and antibacterial properties. *RSC Adv.* 7 (2017) 28670–28676.
3. Kang L, Shi Y, Zhang J, Huang C, Zhang N, He Y, Li W, Wang C, Wu X, Zhou X. A flexible resistive temperature detector (RTD) based on in-situ growth of patterned Ag film on polyimide without lithography. *Microelectron. Eng.* 216 (2019) 111052.
4. Liaw DJ, Wang KL, Huang YC, Lee KR, Lai JY, Ha CS. Advanced polyimide materials: Syntheses, physical properties and applications. *Prog. Polym. Sci.* 37 (2012) 907–974.
5. Ou X, Lu X, Chen S, Lu Q. Thermal conductive hybrid polyimide with ultrahigh heat resistance, excellent mechanical properties and low coefficient of thermal expansion. *Eur. Polym. J.* 122 (2019) 109368.
6. Chen TP, Young SJ, Chang SJ, Hsiao CH. Photoconductive gain of vertical ZnO nanorods on flexible polyimide substrate by low-temperature process. *IEEE Sens. J.* 11 (2011) 3457–3461.
7. Cooper R, Ferguson D, Engelhart DP, Hoffmann R. Effects of radiation damage on polyimide resistivity. *J. Spacecr. Rockets.* 54 (2017) 343–348.
8. Shen FY, Huang SE, Dow WP. Silver metallization of polyimide surfaces using environmentally friendly reducing agents. *ECS Electrochem. Lett.* 2 (2013) 45–48.
9. Chen JJ, An Q, Rodriguez RD, Sheremet E, Wang Y, Sowade E, Baumann RR, Feng ZS. Surface modification with special morphology for the metallization of polyimide film. *Appl. Surf. Sci.* 487 (2019) 503–509.
10. Nguyen THL, Cortes LQ, Lonjon A, Dantras E, Lacabanne C. High conductive Ag nanowire-polyimide composites: Charge transport mechanism in thermoplastic thermostable materials. *J. Non. Cryst. Solids.* 385 (2014) 34–39.
11. Akamatsu K, Ikeda S, Nawafune H. Site-Selective Direct Silver Metallization on Surface-Modified Polyimide Layers. *Langmuir.* 19 (2003) 10366–10371.
12. Tang QY, Chan YC, Wong NB, Cheung R. Surfactant-assisted processing of polyimide/multiwall carbon nanotube nanocomposites formicroelectronics applications. *Polym. Int.* 59 (2010) 1240–1245.
13. Akamatsu K, Shinkai H, Ikeda S, Adachi S, Nawafune H, Tomita S. Controlling interparticle spacing among metal nanoparticles through metal-catalyzed decomposition of surrounding polymer matrix. *J. Am. Chem. Soc.* 127 (2005) 7980–7981.
14. Chang TFM, Wang CC, Yen CY, Chen SH, Chen CY, Sone M. Metallization of polyimide films with enlarged area by conducting the catalyzation in supercritical carbon dioxide. *Microelectron. Eng.* 153 (2016) 1–4.
15. Choi DJ, Maeng JS, Ahn KO, Jung MJ, Song SH, Kim YH. Synthesis of Cu or Cu₂O-polyimide nanocomposites using Cu powders and their optical properties. *Nanotechnology.* 25 (2014), 375604.
16. Kou H, Jia L, Wang C. Electrochemical deposition of flower-like ZnO nanoparticles on a silver-modified carbon nanotube/polyimide membrane to improve its photoelectric activity and photocatalytic performance. *Carbon.* 50 (2012) 3522–3529.
17. Chen Q, Sun Y, Wang Y, Cheng H, Wang QM. ZnO nanowires-polyimide nanocomposite piezoresistive strain sensor. *Sensors Actuators, A Phys.* 190 (2013) 161–167.
18. Babrekar HA, Jejurikar SM, Jog JP, Adhi KP, Bhoraskar SV. Low thermal emissive surface properties of ZnO/polyimide composites prepared by pulsed laser deposition. *Appl. Surf. Sci.* 257 (2011) 1824–1828.
19. Li D, Wu C, Ruan L, Wang J, Qui Z, Wang K, Liu Y, Zhang Y, Guo T, Lin J, Kim TW. Electron-transfer mechanisms for confirmation of contact-electrification in ZnO/polyimide-based triboelectric nanogenerators. *Nano Energy.* 75 (2020) 104818.
20. Shishino K, Yamada T, Arai M, Ikeda M, Hirata H, Motoi M,

- Hatakeyama T, Teshima K. A strongly adhering ZnO crystal layer: Via a seed/buffer-free, low-temperature direct growth on a polyimide film via a solution process. *CrystEngComm*. 22 (2020) 5533-5538.
21. Wu Z, Wu D, Qi S, Zhang T, Jin R. Preparation of surface conductive and highly reflective silvered polyimide films by surface modification and in situ self-metallization technique. *Thin Solid Films*. 493 (2005) 179-184.
 22. Liu TJ, Chen CH, Wu PY, Lin CH, Chen CM. Efficient and Adhesiveless Metallization of Flexible Polyimide by Functional Grafting of Carboxylic Acid Groups. *Langmuir*. 35 (2019) 7212-7221.
 23. Cetinel A, Artunç N, Tarhan E. The growth of silver nanostructures on porous silicon for enhanced photoluminescence: The role of AgNO₃ concentration and deposition time. *EPJ Appl. Phys.* 86 (2019) 11301.
 24. Aydemir G, Utlu G, Çetinel A. Growth and characterization of ZnO nanostructures on porous silicon substrates: Effect of solution temperature. *Chem. Phys. Lett.* 737 (2019) 136827.
 25. Yang J, Wang Y, Kong J, Jia H, Wang Z. Synthesis of ZnO nanosheets via electrodeposition method and their optical properties, growth mechanism. *Opt. Mater.* 46 (2015) 179-185.
 26. Patterson AL. The scherrer formula for X-ray particle size determination. *Phys. Rev.* 56 (1939) 978-982.
 27. Siegel J, Polivková M, Kasálková NS, Kolská Z, Švorčík V. Properties of silver nanostructure-coated PTFE and its biocompatibility. *Nanoscale Res. Lett.* 8 (2013) 1-10.
 28. Sessler GM, Hahn B, Yoon DY. Electrical conduction in polyimide films. *J. Appl. Phys.* 60 (1986) 318-326.